Composition-dependent layered structure and transport properties in BiTe thin films

Yunki Kim, Sunglae Cho,* Antonio DiVenere, George K. L. Wong,† and J. B. Ketterson‡
Department of Physics and Astronomy, Northwestern University, Evanston, Illinois 60208
(Received 20 September 1999; published 26 March 2001)

We have studied the compositional dependence of the layered structure of $Bi_{1+x}Te_{1-x}$ thin films and its relation with the transport properties. We have observed that the $Bi_{1+x}Te_{1-x}$ films have a stable structure near the Bi_1Te_1 composition and that their crystallinity depends strongly upon the compositional deviation from stoichiometric Bi_1Te_1. We have determined possible layered structures, configured with two sequences of Bi–Bi and Te–Bi–Te–Bi–Te, corresponding to Bi and Te binary compositions using x-ray diffraction analysis. Their *c*-axis lattice constants were in the range of 36 Å and 136 Å. Temperature-dependent thermopowers of the films reveal that as the composition changes from Te rich to Bi rich, the polarity varies from *n* type to *p* type.

DOI: 10.1103/PhysRevB.63.155306 PACS number(s): 73.50.Lw, 85.80.Fi

I. INTRODUCTION

In the Bi–Te system, there are several known compounds, with respect to the binary composition, such as Bi_1Te_1, Bi_2Te_3, Bi_2Te, Bi_4Te_3, Bi_3Te_4, Bi_3Te_7, etc. These compounds have been widely investigated because of their unique thermoelectric properties. Among them, Bi_2Te_3 has been used for near-room temperature Peltier-cooling devices. All of these compounds have layered structures with hexagonal symmetry and large *c*-axis lattice constants. Hexagonal Bi_1Te_1, with lattice constants of $a=4.426$ Å, $c=24.069$ Å, is comprised of a Bi–Bi sequence sandwiched between two Te–Bi–Te–Bi–Te sequences, which can be compared with the unit cell of Bi_2Te_3 involving three sequences of Te–Bi–Te–Bi–Te, as shown in Fig. 1.[1] A proposed model for the structure of the Bi–Te system (from Bi to Bi_1Te_3) by Stasova *et al.* combines Bi–Bi and Te–Bi–Te–Bi–Te sequences, i.e., insertion or removal of Bi–Bi layers between Te–Bi–Te–Bi–Te layers.[1,2] There have been many reports on transport properties of the Bi–Te system with respect to binary composition.[3–7] Generally, a small nonstoichiometry from a stable composition in the Bi–Te system is known to have a large doping effect on the transport properties via antisite defect formation: excess Te(Bi) occupies Bi(Te) lattice sites acting as $n(p)$-type dopants.[3–5] Far from stoichiometric combinations, however, there is no consistent explanation for the measured transport data.[6,7] The evolution of the layered structure with compositional change and its relation with the transport properties for large nonstoichiometry have received little attention. Such information is important if one is to optimize the thermoelectric characteristics as well as to understand the nature of the layered structure of these materials.

In this report, we present a systematic study of the compositional dependence of the layered structure of $Bi_{1+x}Te_{1-x}$ thin films and its relation with the transport properties. We have observed that the $Bi_{1+x}Te_{1-x}$ films have a stable structure near the Bi_1Te_1 composition and that their *c*-axis lattice constants vary with the composition. Their transport properties change drastically with the composition.

II. FILM GROWTH AND CHARACTERIZATION

$Bi_{1+x}Te_{1-x}$ films were grown on semi-insulating CdTe(111)B ($a=4.58$ Å) substrates by molecular beam epitaxy (MBE). The in-plane lattice mismatch of Bi_1Te_1 with CdTe(111) is 3.4%. We varied the Bi to Te ratio by changing the deposition rate of the two elements. The base pressure of the growth chamber was in the range of 10^{-10} Torr. The substrates were etched in a solution of 1% bromine in methanol prior to placing them in the load-lock chamber. We first deposited a 3000 Å CdTe buffer layer on the CdTe substrate at 250 °C, followed by the codeposition of Bi and Te at a rate of 0.3–0.4 Å/s. Reflection high-energy electron diffraction (RHEED) was used to examine the specific surface reconstruction, the growth mode, and growth orientation of the deposited layers. The growth temperature of the $Bi_{1+x}Te_{1-x}$ films was 250 °C.

The phase and growth-orientation of the $Bi_{1+x}Te_{1-x}$ thin films were characterized using x-ray diffraction (XRD) including θ–2θ scans and rocking curves. To measure the thermopower, we used the differential method, in which a small temperature difference is maintained across the sample to produce the thermoelectric voltage: $\Delta V(T)=S(T)\nabla T+b(T)(\nabla T)^2+\ldots$, where $b(T)$ is a constant at each temperature T. The thermoelectric voltages, $(\Delta V)_i$, at each temperature difference, $(\nabla T)_i$, were then plotted at a given

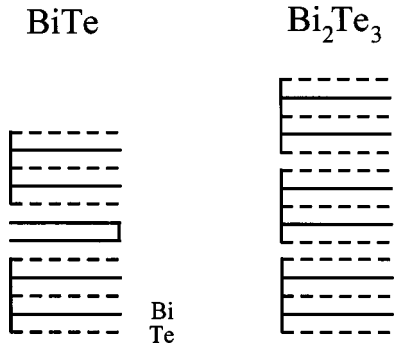

FIG. 1. Schematic diagram of crystal structures of Bi_2Te_3 and BiTe systems. A unit cell of Bi_2Te_3 is composed of three sequences of Te–Bi–Te–Bi–Te. Hexagonal Bi_1Te_1 is made of a Bi–Bi sequence sandwiched between two Te–Bi–Te–Bi–Te sequences.

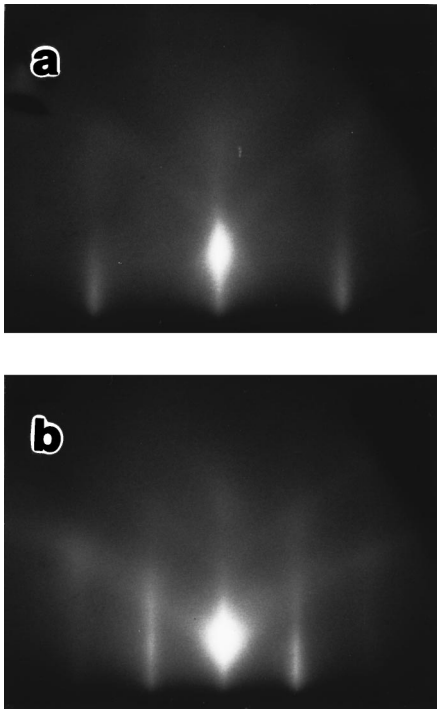

FIG. 2. RHEED patterns of a 3000 Å BiTe film on CdTe(111)B along (a) (10.0) and (b) (12.0) azimuths.

mean temperature, and from the slope of the linear region we could determine the thermopower.[8] For electrical resistivity and Hall measurements, the films were processed into bar-shaped patterns using photolithography and liftoff techniques.

III. RESULTS AND DISCUSSION

Figure 2 shows the RHEED pattern of a 3000 Å $Bi_{1+x}Te_{1-x}$ film on a CdTe(111)B substrate along (10.0) and (12.0) azimuths. The RHEED pattern for the $Bi_{1+x}Te_{1-x}$ films was streaky with Kikuchi lines, representing a layer-by-layer growth. The RHEED patterns repeated every 60°, implying that the $Bi_{1+x}Te_{1-x}$ layers have six-fold in-plane symmetry. No surface reconstruction was observed in the $Bi_{1+x}Te_{1-x}$ growth on CdTe(111)B, even from the initial growth stages. Note that the CdTe(111)B surface has a $2\sqrt{3} \times 2\sqrt{3}$-$R30°$ reconstruction.

Figure 3 shows a θ–2θ XRD pattern of a $Bi_{1+x}Te_{1-x}$ thin film on CdTe(111)B. We have indexed the peaks from the stoichiometric Bi_1Te_1 structure, as shown in the figure. It has (00.1) peaks only, implying *c*-axis oriented growth. There are a couple of small peaks that could not be identified as arising from the Bi_1Te_1, which are also periodic in nature. Assuming that all eight samples have the same structure as Bi_1Te_1, the periodicity of the films can be calculated from the peak position, e.g., (00.5) XRD peak. We define this periodicity as arising from the ''virtual'' *c*-axis lattice constants of the films to distinguish them from the ''actual'' *c*-axis lattice constants; and we use these values to identify our samples. The virtual *c*-axis lattice constants in our samples ranged from 22.36 Å up to 24.85 Å. In order to

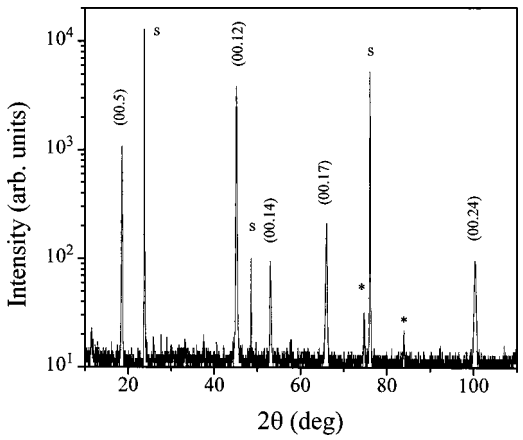

FIG. 3. XRD θ–2θ diffraction patterns of a $Bi_{1-x}Te_{1-x}$ thin film on CdTe(111)B; *s* denotes CdTe substrate peaks. The peaks have been indexed relative to Bi_1Te_1. Note that with this method of indexing there are several unidentified peaks (marked as *).

evaluate the crystallinity of the films, we measured the XRD rocking curve (i.e., we performed an ω scan)[9] and determined the full width at half-maximum (FWHM) at the Bi_1Te_1 (00.12) peak. Figure 4 shows FWHM with respect to the virtual *c*-axis lattice constants of the $Bi_{1+x}Te_{1-x}$ films. Near the Bi_1Te_1 position, the FWHM value was measured to be 0.193°. Deviations from stoichiometric Bi_1Te_1 result in an increase in the FWHM; it goes up to 0.813° and 0.332° for the Bi-rich and Te-rich compositions, respectively. The fact that the FWHM reaches a minimum when the virtual *c*-axis lattice constant approaches the bulk value of Bi_1Te_1 suggests that Bi_1Te_1 has a stable structure near the stoichiometric composition.

We now address the origins of the virtual *c*-axis lattice constant change for the Bi- and Te-rich compositions and the presence of unidentified peaks. In Te-rich Bi_2Te_3 thin films,

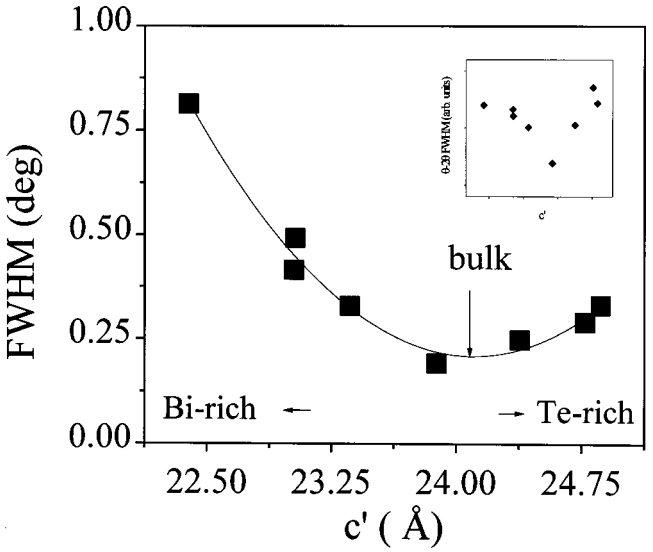

FIG. 4. Rocking curve FWHM values at the (00.12) peaks versus the virtual *c*-axis lattice constant (c') of $Bi_{1+x}Te_{1-x}$ thin films. Crystallinity becomes worse when the composition deviates from the stoichiometric Bi_1Te_1.

TABLE I. XRD data and the calculated structural parameters of $Bi_{1+x}Te_{1-x}$ thin films. The virtual *c*-axis lattice constants (c') calculated using the assumption that all the films have the same structure as Bi_1Te_1, have been obtained from the peaks near the BiTe (00.5). From a fit that makes the values of $l=2c\sin\theta/\lambda(=c/d)$ integers for all the peak positions in the XRD pattern, the actual *c*-axis lattice constant (c) and (00.l) positions have been determined. An error function (δ) is defined by $\sqrt{\Sigma_i^N[l_i-\text{nearest-integer}(l_i)]^2}/N$, where N is the number of measured peaks for the sample and i is a dummy index.

c' (Å)	*d* spacing at each XRD peak (Å)/calculated index *l*											δ	c (Å)
22.36	4.471/8	3.567/10	3.247/11	2.247/16	1.990/18	1.785/20		1.381/26	1.279/28		0.9956/36	0.0136	35.82
23.02	4.618/13	3.521/17		2.302/26	1.997/30	1.763/34		1.393/43	1.275/47	1.175/51	0.9987/60	0.00501	59.92
23.03	4.595/19	3.507/25		2.308/38	1.995/44	1.756/50	1.566/56	1.394/63	1.273/69	1.171/75	0.9983/88	0.0138	87.80
23.36	4.672/29	3.480/39	3.234/42	2.341/58	1.999/68	1.742/78	1.618/84	1.402/97	1.271/107	1.161/117	1.0000/136	0.0173	135.9
23.88	4.776/13				2.007/31	1.727/36		1.414/44	1.269/49	1.152/54	1.003/62	0.00570	62.19
24.07	4.782/5				2.001/12	1.720/14		1.416/17			1.003/24	0.00894	24.07
24.38	4.876/12		3.232/18		2.015/29	1.712/34		1.427/41	1.269/46		1.007/58	0.0243	58.40
24.79	4.959/24				2.015/59	1.697/70		1.432/83			1.007/118	0.0108	118.8
24.85	4.970/13	3.405/19			2.002/32	1.702/38		1.439/45	1.269/51	1.135/57	1.012/64	0.00665	64.72

we have observed that the antisite defects induce reduced *c*-axis lattice constants because of the smaller Te atomic radius (Bi: 1.6 Å, Te: 1.4 Å).[5] However, Bi_1Te_1 shows the opposite behavior: the Te-rich side has larger *c*-axis lattice constants than the Bi-rich side. Thus the antisite defect can be excluded as the main cause of the virtual *c*-axis lattice constant behavior. One way to account for this phenomena is to describe the crystal structures as a combination of Bi–Bi and Te–Bi–Te–Bi–Te sequences, as proposed by Stasova *et al.*[1,2] As the BiTe system departs from the Bi_1Te_1 stoichiometric composition, one of the two sequences, Bi–Bi for the Bi-rich side or Te–Bi–Te–Bi–Te for the Te-rich side, will be inserted periodically with a little randomness, resulting in a new hexagonal phase with different *c*-axis lattice constants. One explanation of the FWHM behavior can be structural disorder involving a nonperiodic insertion/removal of the Bi–Bi sequence in the Te–Bi–Te–Bi–Te sequences due to a deviation from the stable structure. This is reinforced by the fact that the FWHM of the Bi_1Te_1 (00.12) peak in the θ–2θ scan shows a similar behavior, as shown in the inset of Fig. 4. The θ–2θ scan can give information on the structural deviations along the outward surface normal of the sample a little more precisely than the ω scan.

From the periodic XRD peaks and the six-fold symmetric RHEED patterns, we considered all the XRD peaks (00.l). In Table I, *d* spacings of all of the XRD peaks of our eight samples are given. In order to obtain information on the structure of the samples, we made a fit for which all values $l=2c\sin\theta/\lambda(=c/d)$ are integers, where c is the *c*-axis lattice constant, λ is the x-ray wavelength (1.54056 Å), d is the *d* spacing, and l is the index number along the *c*-axis in the hexagonal crystal structure. We define c as the actual *c*-axis lattice constant to compare with c', the virtual *c*-axis lattice constant. By searching for the value of c that makes the error function of the difference between l and the nearest integer of l a minimum for all XRD peak positions in a sample, we have obtained the optimum integers l's and the real *c*-axis values. The actual *c*-axis lattice constants are in the range of 36 Å–136 Å, as shown in Table I. For comparison, literature values of the XRD peaks and *c*-axis lattice constant of bulk Bi_1Te_1 are listed in the sixth row in Table I.

Additional structural aspects are shown in Table II. The configuration of sequences and the composition of Bi and Te were calculated based on Stasova *et al.*'s model in which Bi–Bi sequences are inserted or removed between Te–Bi–Te–Bi–Te sequences for each sample with a different *c*-axis lattice constant. The suggested numbers of the sequences, α and β of $(\text{Te–Bi–Te–Bi–Te})_\alpha(\text{Bi–Bi})_\beta$,[11] are listed in Table II, the corresponding numbers x and y of the compositional ratio of Bi and Te in Bi_xTe_y films are also listed. The fitted results indicate that the Te compositions of our samples ranged from 33% to 56%. In Fig. 5, schematic diagrams of suggested structures for the Bi_xTe_y thin films are shown for eight configurations: (2,1), (3,2), (13,9), (19,15), (16,15), (14,15), (26,33), (14,18), and for reference (1,1). The *c*-axis lattice constants of the films are scattered and larger than that of Bi_1Te_1. We may conclude from these results that in the Bi- or Te-rich BiTe system, the structural configuration is unique and strongly related to the composition and possibly predictable for a specific composition, as discussed for the Bi–Se system.[1]

TABLE II. XRD data and calculated structural parameters of $Bi_{1+x}Te_{1-x}$ thin films. Here c' and c are the virtual *c*-axis lattice constants and the actual *c*-axis lattice constants, respectively. The suggested numbers of sequences, α and β of $(\text{Te–Bi–Te–Bi–Te})_\alpha(\text{Bi–Bi})_\beta$, are also listed. The numbers x and y are the compositional ratio of Bi and Te in Bi_xTe_y films in a unit cell.

c' (Å)	$(\text{Te–Bi–Te–Bi–Te})_\alpha(\text{Bi–Bi})_\beta$ $\sim(\alpha,\beta)$	Bi_xTe_y $\sim(x,y)$	c (Å)
22.36	(2,4)	(2,1)	35.82[10]
23.02	(4,5)	(3,2)	59.92
23.03	(6,7)	(13,9)	87.80
23.36	(10,9)	(19,15)	135.9
23.88	(5,3)	(16,15)	62.19
24.07	(2,1)	(1,1)	24.07
24.38	(5,2)	(14,15)	58.40
24.79	(11,2)	(26,33)	118.8
24.85	(6,1)	(14,18)	64.72

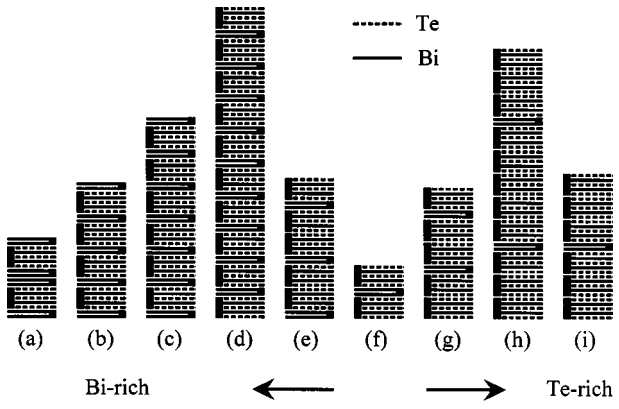

FIG. 5. Schematic diagram of suggested structures for the Bi_xTe_y thin films; $(x,y)=$(a) (2,1), (b) (3,2), (c) (13,9), (d) (19,15), (e) (16,15), (f) (1,1), (g) (14,15), (h) (26,33), and (i) (14,18).

In order to investigate transport properties for the eight different structural configurations, we have measured thermopowers between 20 and 300 K, as shown in Fig. 6(a). There was a drastic change in the thermopowers of the films with respect to the composition of Bi and Te. The thermopower curves of the $Bi_{1+x}Te_{1-x}$ films show an almost linear temperature dependence, characteristic of degenerate behavior. The thermopowers of the Bi-rich BiTe films (with smaller virtual *c*-axis lattice constants) display *p*-type behavior, whereas those of the Te-rich BiTe films (with larger virtual *c*-axis lattice constants) display *n*-type behavior. The resistivity of a $Bi_{16}Te_{15}$ film displays a linear temperature dependence. The electron density and mobility at room temperature are $1.2\times10^{20}\,cm^{-3}$ and 45.8 $cm^2/V\,s$, respectively, as determined from Hall and resistance measurements. The thermopowers of the films at room temperature with respect to the virtual *c*-axis lattice constants are shown in Fig. 6(b). This figure shows an abrupt change of thermopower values, from negative to positive, near the transition from Te rich to Bi rich, although the point of the polarity change is slightly shifted from the Bi_1Te_1 stoichiometric composition. This result might be a characteristic of its layered structure, not a doping effect, because the magnitudes of thermopower values are almost invariant with compositional deviation. In a Te-rich Bi_2Te_3 film, we have observed that a small nonstoichiometry has large *n*-type doping effect on the transport properties via antisite defect formation, resulting in the reduced magnitude of thermopower with increased Fermi level.[5] These results suggest that the layered structure in the Bi–Te system is strongly related to the composition and has a great effect on the electronic properties. The easy controllability of *n*- and *p*-type thermopower characteristics (by changing the binary composition) in the Bi–Te system suggests this material could be considered as a possible thermoelectric element.

IV. SUMMARY

Thin films of hexagonal $Bi_{1+x}Te_{1-x}$ have been grown on CdTe(111)B substrates using MBE. XRD studies shows that

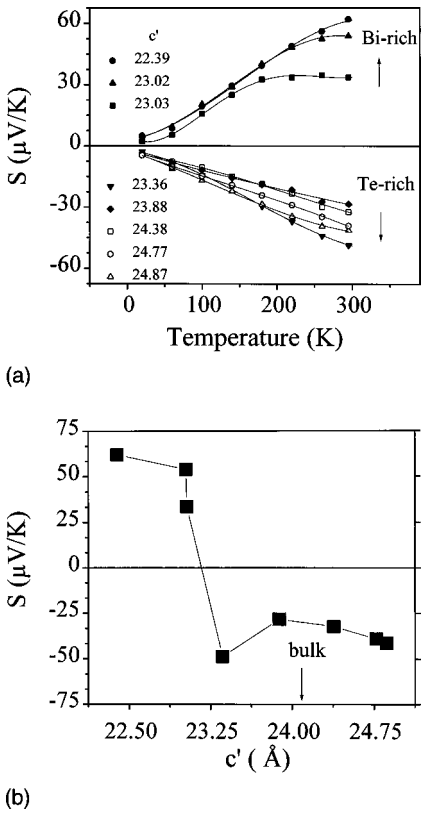

FIG. 6. (a) Temperature-dependent thermopowers of the $Bi_{1+x}Te_{1-x}$ thin films. (b) Room temperature thermopowers with respect to virtual *c*-axis lattice constants (c') of the films.

the $Bi_{1+x}Te_{1-x}$ films have a stable and highly periodic structure near the Bi_1Te_1 composition. Their crystallinity depends strongly upon the compositional deviation from stoichiometric Bi_1Te_1, due to structural disorder by the nonperiodic insertion/removal of the Bi–Bi sequences in the Te–Bi–Te–Bi–Te sequences. From the x-ray analysis, possible layered structures using two sequences of Bi–Bi and Te–Bi–Te–Bi–Te at each composition have been determined, supporting the model by Stasova. Their *c*-axis lattice constants were in the range of 36 Å–136 Å. Their transport properties change drastically with the composition. Temperature-dependent thermopower measurements on the films reveal that as the composition changes from Te rich to Bi rich, the thermopower varies from *n* type to *p* type, characteristic of their layered structures. These results suggest that the layer structure in the Bi–Te system is strongly dependent on the composition and has a great effect on the electronic properties.

ACKNOWLEDGMENTS

This work was supported by DARPA under Grant No. DAAG55-97-1-0130. Use was made of MRL Central Facilities supported by the National Science Foundation, at the Materials Research Center of Northwestern University, under Award No. DMR-9120521.

*Permanent address: Department of Physics, University of Ulsan, Ulsan, South Korea.

†Permanent address: Physics department, HKUST, Clearwater Bay, Kowloon, Hong Kong, China.

‡Also at Department of Electrical and Computer Engineering, Northwestern University, Evanston, Illinois 60208.

[1] M. M. Stasova, Zh. Strukt. Khim. **8**, 655 (1967) [J. Struct. Chem. **8**, 584 (1967)]; **5**, 793 (1964); [J. Struct. Chem. **5**, 731 (1964)]; M. M. Stasova and O. G. Karpinskii, *ibid.* **8**, 85 (1967) [J. Struct. Chem. **8**, 69 (1967)].

[2] P. M. Imamov and S. A. Semiletov, Kristallografiya **15**, 972 (1971) [Sov. Phys. Crystallogr. **15**, 845 (1971)].

[3] T. C. Harman, S. E. Miller, and H. L. Goeing, Bull. Am. Phys. Soc. **30**, 35 (1955).

[4] E. Charles, E. Groubert, and A. Boyer, J. Mater. Sci. Lett. **7**, 575 (1988).

[5] S. Cho, Y. Kim, A. DiVenere, G. K. Wong, and J. B. Ketterson, Appl. Phys. Lett. **75**, 1401 (1999).

[6] M. J. McCulley, G. W. Neudeck, and G. L. Liedl, J. Vac. Sci. Technol. **10**, 391 (1973).

[7] M. M. Ibrahim, N. Afify, M. M. Hafiz, and M. A. Mahmoud, J. Phys. Chem. Solids **51**, 253 (1990).

[8] S. Cho, A. DiVenere, G. K. Wong, J. B. Ketterson, J. R. Meyer, and C. A. Hoffman, Solid State Commun. **102**, 673 (1997).

[9] We express the deviation of the scattered x-ray vector from the reciprocal lattice point by an angle α measured with respect to the outward surface normal of the sample, where $\alpha = 90 - \psi$, and ψ follows from $\Delta\omega = 2\Delta\theta/(1 + \cot\theta_B \cot\psi)$ which is Eq. (2) of C. R. Wie, Mater. Sci. Eng., R. **13**, 1 (1994); here $\Delta\omega$ is the variation in the scattering angle from the crystal, $\Delta\theta$ is the variation in the incident angle, and θ_B is the Bragg angle. We used double-crystal x-ray diffraction with a slit whose acceptance angle is 0.2°. In this configuration, the angle α can be calculated as a function of the Bragg angle and the rotation angle, ω, of the sample. For $\theta_B = 22.5°$ and $\omega = 0.5°$, $59° < \alpha < 90°$.

[10] Synthetic bulk Bi_2Te_1 (Ref. 1) has a unit cell of half of this value. The value chosen for this study yielded the best fit in the *c*-axis lattice constant calculation using the measured XRD data.

[11] If the stacking sequence of the $Bi_{1+x}Te_{1-x}$ films follows the rule A, B, C, A, B, C,... as in fcc cubic crystal, which is the case for Bi_2Te_3, then the number of atomic layers in a unit cell should be a multiple of three and the unit cells of some of our samples whose number of layers are not multiples of three should be tripled.